

Akzeptierter Artikel

Titel: The energetics of mesopore formation in zeolites with surfactants

Autoren: Noemi Linares, Erika de Oliveira Jardim, Alexander Sachse, Elena Serrano, and Javier Garcia-Martinez

Dieser Beitrag wurde nach Begutachtung und Überarbeitung sofort als "akzeptierter Artikel" (Accepted Article; AA) publiziert und kann unter Angabe der unten stehenden Digitalobjekt-Identifizierungsnummer (DOI) zitiert werden. Die deutsche Übersetzung wird gemeinsam mit der endgültigen englischen Fassung erscheinen. Die endgültige englische Fassung (Version of Record) wird ehestmöglich nach dem Redigieren und einem Korrekturgang als Early-View-Beitrag erscheinen und kann sich naturgemäß von der AA-Fassung unterscheiden. Leser sollten daher die endgültige Fassung, sobald sie veröffentlicht ist, verwenden. Für die AA-Fassung trägt der Autor die alleinige Verantwortung.

Zitierweise: *Angew. Chem. Int. Ed.* 10.1002/anie.201803759
Angew. Chem. 10.1002/ange.201803759

Link zur VoR: <http://dx.doi.org/10.1002/anie.201803759>
<http://dx.doi.org/10.1002/ange.201803759>

The energetics of mesopore formation in zeolites with surfactants

N. Linares, E. O. Jardim, A. Sachse, E. Serrano, and J. García-Martínez*

Abstract: Mesoporosity can be conveniently introduced in zeolites by treating them in basic surfactant solutions. The apparent activation energy involved in the formation of mesopores in USY via surfactant-templating was obtained through the combination of *in situ* synchrotron XRD and *ex situ* gas adsorption. Additionally, techniques such as pH measurements and TG/DTA were employed to determine the OH⁻ evolution and the CTA⁺ uptake during the development of mesoporosity, providing information about the different steps involved. By combining both *in situ* and *ex situ* techniques, we have been able, for the first time, to determine the apparent activation energies of the different processes involved in the mesostructuring of USY zeolites, which are in the same order of magnitude (30 – 65 kJ mol⁻¹) of those involved in the crystallization of zeolites. Hence, important mechanistic insights on the surfactant-templating method were obtained.

For more than 25 years now, cationic surfactants have been widely applied to prepare mesoporous amorphous materials.^[1,2] Since then, researchers have made great efforts to extend the use of these surfactant-templating techniques for the preparation of mesoporous zeolites. Among the different methods used to impart secondary porosity within zeolites,^[3,4] the post-synthetic treatment with cationic surfactants has proved to be an effective tool to introduce tunable intracrystalline mesoporosity while maintaining the key features of the zeolite including strong acidity and excellent hydrothermal stability.^[5,6] Recently, we reported the first time-resolved observation of the development of mesoporosity in zeolites through surfactant-templating by *in situ* XRD.^[7] Indeed, the combination of experimental data with theoretical calculations provided new insights on the formation of intracrystalline mesoporosity featuring short-range order in zeolites. Moreover, the use of Liq-TEM rendered the first *in situ* real time visualization of this process.^[7]

In spite of the numerous reports dealing with surfactant-templating of zeolites^[5-7] and the fact that these materials are already a commercial reality,^[8] the driving forces responsible for this process are still unknown. Their investigation is one of the objectives of this paper. A systematic study of the apparent activation energies of the different processes involved in surfactant-templating in zeolites was undertaken to increase our

understanding of this approach. With this aim, *in situ* synchrotron XRD and SAXS studies of this process were performed using the experimental setup shown in Figure 1a. This apparatus was specifically designed and built to get detailed information about the kinetics of the surfactant-templating process, as it allows for the *in situ* monitoring of the pH and temperature while performing the XRD and SAXS measurements. The reaction mixture, containing the basic surfactant solution ([NaOH] = 0.09 M; [CTAB] = 0.07 M) was placed in a sealed reactor while the temperature was carefully controlled (± 0.1 °C) in the 45 – 90 °C range. The USY zeolite (CBV 720, Si/Al = 15) was introduced in the addition vessel on top of the reactor. The programmed opening of the lid between the reactor and the vessel allowed for the addition of the zeolite at once and thus the collection of data from the beginning of the reaction. Both pH and temperature probes were fitted in the reactor in order to continuously monitor both parameters. A peristaltic pump was used to circulate the mixture through a capillary where both the XRD and SAXS measurements were realized (see Figure S1 for further details).

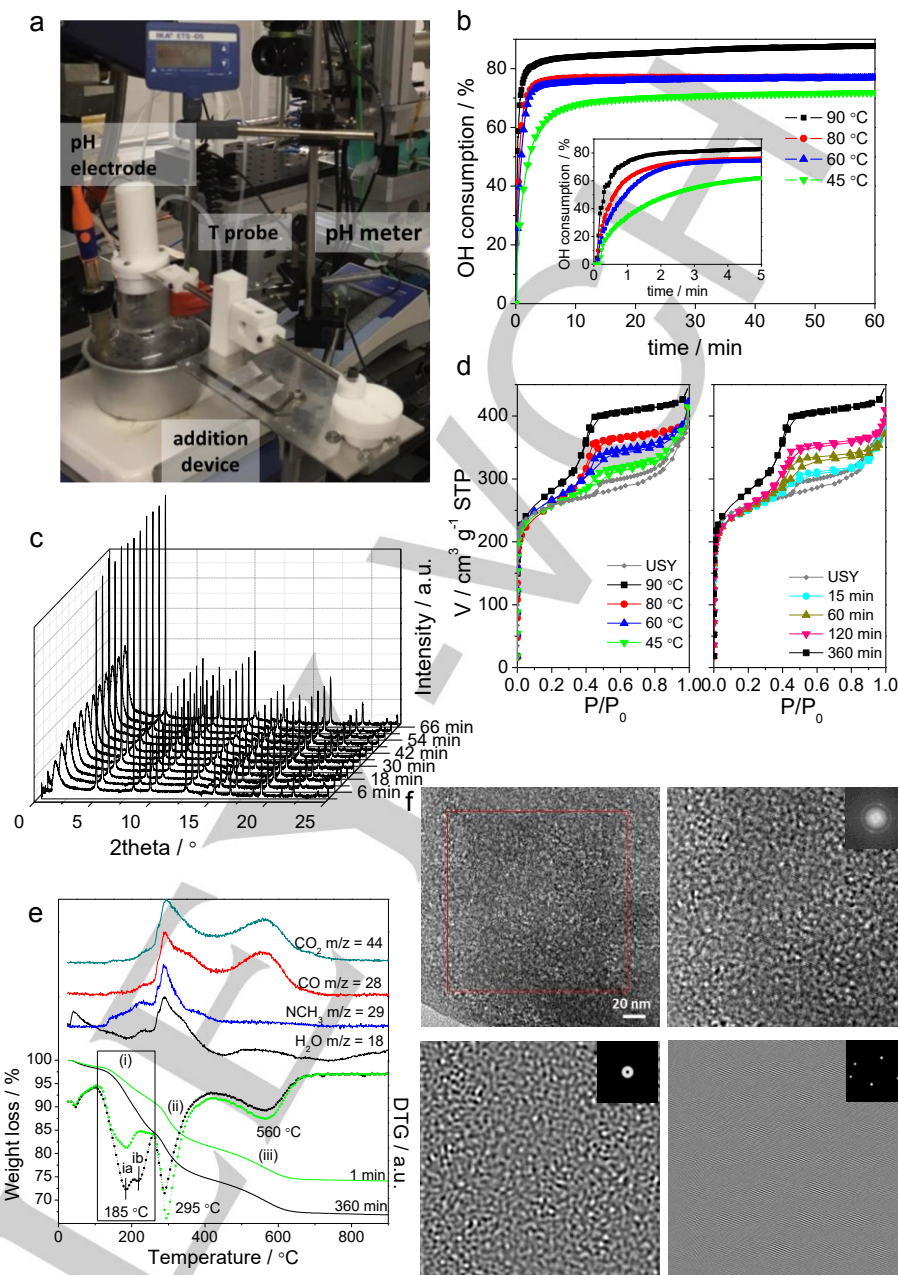
The evolution of the pH was *in situ* monitored (Figure S2a) providing kinetic information on the OH⁻ consumption. These experiments were carried out after calibrating the pH glass electrode with titrated NaOH solutions at the different temperatures studied, see ESI and Figure S3 for details.^[9] The decrease of the OH⁻ concentration is due to both the cleaving of Si-O-Si bonds^[9] and the ion exchange between H⁺ and Na⁺/CTA⁺ ions in the zeolite. To distinguish between both processes, experiments in which the zeolite was firstly converted into its Na-form were carried out (Figure S2b) thus avoiding the ion exchange by H⁺ ions during surfactant-templating. Similar results were obtained in both cases (Figure S2) and thus experiments obtained from the Na-form of the zeolite were employed in this case (Figure 1b). As deduced from the consumption of OH⁻ the cleavage of the Si-O-Si bonds is a very fast process, occurring within the first 5 min of the treatment (Figure 1b). As previously described,^[10] the opening of the Si-O-Si bonds and the formation of SiO⁻ sites is required for the mesostructuring to occur. Indeed, the process does not take place if base is not added to the reaction media (Figure S4) and the initial [OH⁻] determines the amount of mesoporosity that can be formed within the zeolite.^[10]

In order to obtain the apparent activation energy of the cleavage of the Si-O-Si bonds, its rate constant, *k*, at different temperatures was determined from the slope of the linear part of the evolution of [OH⁻] versus time. These values were used to depict the Arrhenius plot, from where the Arrhenius apparent activation energy was obtained, $E_a^{\text{OH}^-} = 35 \text{ kJ mol}^{-1}$ (Figure 2b, OH⁻ data). After that, the step related to the surfactant uptake by the zeolite was investigated by TG to determine the amount of CTA⁺ incorporated.

- [a] Dr. N. Linares, Dr. E. O. Jardim, Dr. A. Sachse, Dr. E. Serrano, and Prof. Dr. J. García-Martínez
Laboratorio de Nanotecnología Molecular, Departamento de Química Inorgánica
Universidad de Alicante
Ctra. San Vicente-Alicante s/n, E-03690 Alicante, Spain.
E-mail: j.garcia@ua.es; www.nanomol.es
- [b] Prof. Dr. J. García-Martínez
Rive Technology, Inc.
1 Deer Park Drive, Monmouth Junction, New Jersey 08852, United States

Supporting information for this article is given via a link at the end of the document.

Figure 1. (a) Device used at the ALBA synchrotron, for both the *in situ* synchrotron XRD and SAXS measurements (beamlines BL04-MSPD and BL11-NCD, respectively). *Ex situ* experiments were also performed using this device. Evolution of the different parameters monitored during surfactant-templating of USY zeolite ([CTAB] = 0.07 M and [NaOH] = 0.09 M); (b) OH⁻ consumption profiles at different temperatures; (c) *in situ* time resolved synchrotron XRD patterns at 90 °C; (d) N₂ adsorption/desorption isotherms at -196 °C for the surfactant-templated USY zeolites at different temperatures and 360 min of treatment (left) and at different times at 90 °C (right); (e) TG-DTG/MS measurements at the beginning (1 min) and the end (360 min) of the treatment at 90 °C. The TGA (solid line) is presented below along with the DTG data (dashed line). Above are plotted various molecular species recorded from the MS measurements and their evolution with temperature; (f) (top left) TEM image of an ultramicrotomed surfactant-templated USY zeolite after 360 min of treatment at 90 °C, (top right) reconstruction of the area marked by the red square from its corresponding FFT pattern (inset), (bottom left) mesopore structure of the selected area produced by masking the halo of the FFT pattern (inset) and (bottom right) crystalline structure of the area produced by masking the spots of the FFT pattern (inset).



As an example, Figure 1e shows the TG-DTG/MS data of USY zeolite at the beginning (1 min, green line) and the end (360 min, black line) of the surfactant-templating treatment at 90 °C. The calcination of CTA⁺ in mesoporous materials involves three steps: (i) the elimination of the trimethylamine head group via Hofmann degradation (< 250 °C); (ii) the oxidation of organic components (< 400 °C), and (iii) a final oxidation process (> 400 °C) during which carbonaceous species are removed.^[11] These three steps were observed in the TG-DTG/MS plots of surfactant-templated zeolites but also in those of a control experiment in which no base was added to the solution (Figure S5a) and of a physical mixture of zeolite and CTAB (Figure S5b). However, only when both the surfactant and the base are present, and therefore the mesostructuring of the zeolite occurs, the peak corresponding to the first step (i) increases with the time of treatment, as shown in Figure 1e. When no base is used in the treatment, no mesostructuring of the zeolite occurs, and therefore the intensity of this peak remains nearly constant, see Figure S5a. Hence, the amount of CTA⁺ removed in this first step (i) was associated to the CTA⁺ responsible for the mesostructuring of the zeolite (more details

are given in the ESI). Selected experiments were repeated at least twice to confirm the reproducibility of these results. As an example, the standard deviation of the uptake of CTA⁺ associated to the SiO⁻ sites at 45 °C was found lower than 2% (three repetitions). Therefore, the percentage of CTA⁺ removed in (i) (Figure S6) was used to determine the apparent activation energy of the process involving the uptake of CTA⁺ associated to the SiO⁻ sites (Figure 2b, CTA⁺ data), $E_a^{\text{CTA}^+} = 29 \text{ kJ mol}^{-1}$. Up to now, we have determined the apparent activation energy of two intermediate steps involved in the surfactant-templating of zeolites (see Figure 3). Following, the apparent activation energy for the whole surfactant-templating process was calculated using two independent techniques, namely, low angle XRD and N₂ physisorption.

In situ synchrotron XRD experiments were performed using the experimental setup shown in Figure 1a. Diffractograms were recorded from 0.35 to $40^\circ 2\theta$ with time intervals of 2 min, allowing for the concurrent study of the kinetics of both the development of mesoporosity and the evolution of the crystallinity of the samples throughout the surfactant-templating of the zeolite. The evolution of the mesoporosity was inferred from the evolution of the peak in the low angle region of the diffractogram, at $1.6^\circ 2\theta$, whose intensity increases throughout the experiment before reaching a plateau, indicating the completion of the mesostructuring process.^[7] In this study, mild reaction conditions were used to follow the early stages of this process with higher accuracy. As an example, Figure 1c shows the *in situ* time resolved synchrotron XRD patterns of USY zeolite during surfactant-templating at 90°C , after a stable signal is reached. While the $1.6^\circ 2\theta$ peak evolves with time, the crystallinity of the zeolite remains almost constant from the beginning of the treatment (see Figure 1c). The intensity of the peak at $1.6^\circ 2\theta$ increases linearly with time, allowing for the calculation of the rate constant, k' , of the mesostructuring process at different temperatures (Figure 2a). These values were used to produce the Arrhenius plot shown in Figure 2b, from where the apparent activation energy of the development of mesoporosity was obtained, $E_a^{\text{I meso}} = 45 \text{ kJ mol}^{-1}$. The use of the Avrami equation yielded a very similar apparent activation energy, namely 48 kJ mol^{-1} (see ESI and Figure S7 for details). Interestingly, this apparent activation energy is within the range of those obtained by measuring the linear growth rates of zeolites A (47.3 kJ mol^{-1}),^[13a] X (62.6 kJ mol^{-1}),^[13b] Y ($49\text{--}65 \text{ kJ mol}^{-1}$),^[13c] and silicalite-1 (42 kJ mol^{-1}),^[13d] indicating that the energy necessary for the crystallization of the zeolites is similar to the one required for their mesostructuring via surfactant-templating (see Figure 3). These results confirm that the mesostructuring of the USY zeolite (i.e. the controlled formation of highly tunable mesoporosity by surfactant-templating) is energetically feasible under typical conditions of time and temperature involved in the synthesis of zeolites. It is worthy to mention also that the transformation of faujasite into other structures by zeolite interconversion is well-known and involves little energy, as measured by calorimetry.^[14] Exhaustive TEM analysis confirmed the exclusive presence of intracrystalline mesoporosity and discarded the formation of amorphous phases (see Figure 1f). The formation of mesoporosity in zeolites can also be evaluated through *ex situ* N_2 physisorption at 77 K of samples prepared using the same experimental setup at different times and subsequently calcined (see Figure 1d for their isotherms and Figure S8 for the evolution of their mesopore volume). In order to assess the reproducibility of these measurements, the experiments were carried out at least twice obtaining similar results (see representative examples in Figure S9). The differences between the mesopore volumes values found in the repetitions were lower than 10%.

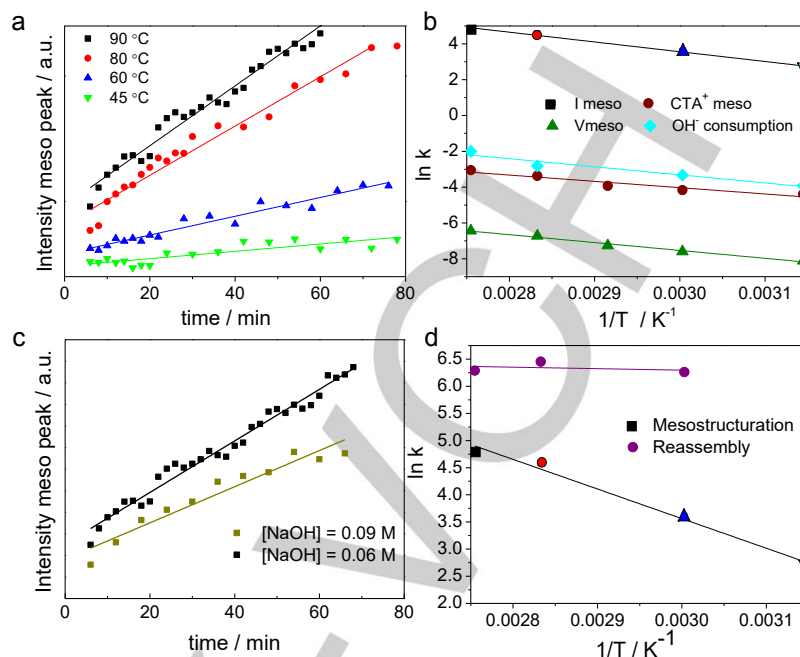


Figure 2. (a) Intensity profiles of the peak at $1.6^\circ 2\theta$ (mesoporosity) during surfactant-templating at different temperatures (0.09 M NaOH). (b) Arrhenius plots obtained from the evolution of the different parameters associated to the development of mesoporosity in a surfactant-templated USY zeolite at 90°C (0.09 M NaOH). (c-d) Intensity profiles of the peak at $1.6^\circ 2\theta$ (mesoporosity) during surfactant-templating at 90°C and different NaOH concentrations, and (d) Arrhenius plots obtained from the I_{meso} profiles of the $1.6^\circ 2\theta$ peak, comparison between surfactant-templating and dissolution + reassembly approaches (0.09 M NaOH).

The kinetics of the development of mesoporosity in USY zeolite measured by gas adsorption is very similar to the one determined by *in situ* XRD measurements (Figure 2b), $E_a^{\text{V meso}} = 43 \text{ kJ mol}^{-1}$ vs $E_a^{\text{I meso}} = 45 \text{ kJ mol}^{-1}$, respectively. The similarity between the apparent activation energies associated to the development of mesoporosity obtained by two independent techniques, XRD and gas adsorption, nicely supports the validity of these results.

In order to obtain further insights into the driving forces of the formation of intracrystalline mesoporosity in zeolites by surfactant-templating, *in situ* synchrotron XRD experiments were performed using different initial NaOH concentrations (0.06 and 0.09 M) and zeolites with varying Si/Al ratios (Si/Al = 15 and 40). As we have previously reported,^[10] the initial OH^- concentration plays a major role in the incorporation of mesoporosity in the zeolite. Indeed, decreasing the initial NaOH concentration by two thirds (0.06 vs 0.09 M) decreases the rate of the development of mesoporosity almost in the same proportion at 90°C , see Figure 2c. On the contrary, zeolites with higher Si/Al ratios result in faster rates, see Figure S10. The stability of the zeolite towards basic cleavage increases with the Al content in the framework,^[10] which results in rates almost 9 times slower for CBV 720 (Si/Al = 15) than CBV 780 (Si/Al = 40) at 60°C . In addition to the *in situ* XRD study, the transformation was also monitored by *in situ* SAXS using the same experimental setup to follow the development of surfactant-templated mesoporosity.

Similar results were obtained, which confirmed the slower kinetics of the surfactant-templating process in zeolites with higher Al content (see Figure S11).

Finally, we compared the kinetics of surfactant-templating with other well known procedure that also uses CTAB and a base, namely, dissolution and reassembly,^[15] to better understand the differences between both methods. First, the dissolution step was carried out in USY zeolite (Si/Al = 15) using a basic solution ([NaOH] = 0.09 M) without the presence of surfactant. The evolution of the concentration of OH⁻ was measured in order to study the cleavage of Si-O-Si bonds in the zeolite (Figure S12). When CTA⁺ is not present, the apparent activation energy obtained ($E_a^{\text{OH-dis}} = 20 \text{ kJ mol}^{-1}$, Figure S12b) is smaller than the one determined during surfactant-templating ($E_a^{\text{OH}^-} = 35 \text{ kJ mol}^{-1}$), see Figure 3. The higher activation energy obtained in the presence of the surfactant is consistent with the high values reported for the dissolution of zeolites in the presence of quaternary amines.^[16] It is well-known that quaternary amines have a protective role towards the desilication of zeolites.^[7,17] This phenomenon is very obvious when comparing the rapid decrease in the intensity of the high-angle XRD peaks of the USY treated in a 0.09 M NaOH solution (blue lines in Figure S13) with the much slower when the surfactant is present (Figure 1c). In the second step (reassembly), CTAB was added to the mixture after 30 minutes of basic treatment. At this point, the dissolved fragments precipitate immediately producing a very intense peak in the low angle region of the X-ray diffractogram (Figure S10, black lines). Moreover, the calculated rate of this second step barely changes with temperature, resulting in very low apparent activation energy ($E_a^{\text{meso reass.}} < 1 \text{ kJ mol}^{-1}$) (Figure 2b). This is consistent with the very low energetic requirement associated to the formation of surfactant-templated silicas.^[18] The very different apparent activation energies of surfactant-templating and dissolution-reassembly suggest that the involved mechanisms are markedly different (Figure 3). This conclusion is further confirmed by the different textural and chemical properties of the materials obtained from both processes.^[10]

From all the abovementioned results and discussion, we have drawn the following conclusions:

(i) The formation of negatively charged Si-O⁻ species by OH⁻ ions is a very fast process that, however, presents a significant apparent activation energy ($E_a^{\text{OH}^-} = 35 \text{ kJ mol}^{-1}$) due to the cleavage of Si-O-Si bonds.

(ii) The incorporation of CTA⁺ in the zeolite is carried out in a two stage process. First, a very fast uptake of the surfactant by the zeolite surface takes place. After that, the CTA⁺ associated to the negatively charged Si-O⁻ sites in the zeolite increases more slowly as the CTA⁺ diffuses through the zeolite porosity. This electrostatic driven process is a less impeded step and presents a lower apparent activation energy, $E_a^{\text{CTA}^+} = 29 \text{ kJ mol}^{-1}$.

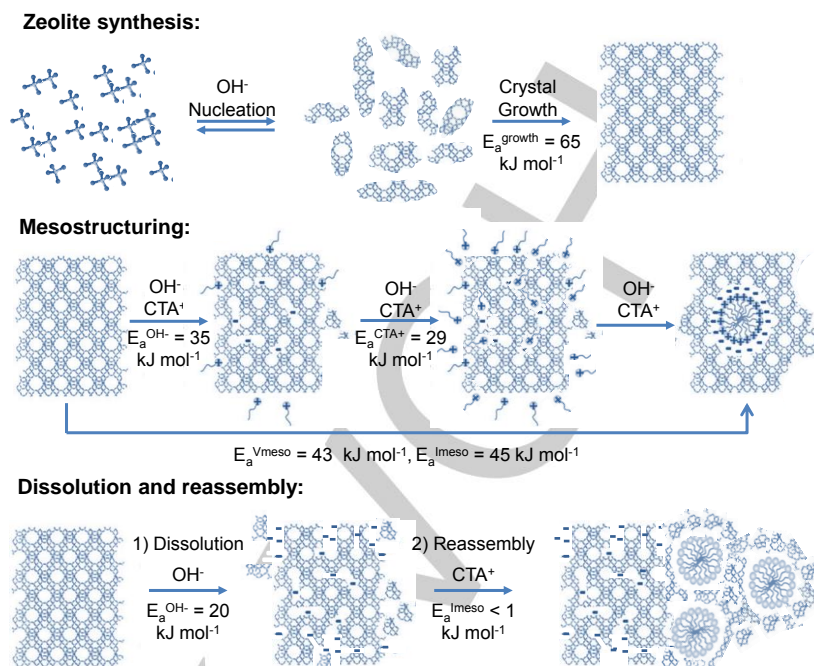


Figure 3. Schematic representation of the different procedures with USY zeolite namely, synthesis^[13c] (above), mesostructuring (centre) and dissolution and reassembly (bottom), and the apparent activation energies of every process involved.

(iii) The kinetics of the whole process, which also involves the formation of CTA⁺ micelles within the zeolite crystals and the rearrangement of the crystal structure to accommodate them, is highly dependent on the temperature, consequently resulting in a higher apparent activation energy, $E_a^{\text{Imeso}} = 45 \text{ kJ mol}^{-1}$ and $E_a^{\text{Vmeso}} = 43 \text{ kJ mol}^{-1}$. Interestingly, these values, which are obtained using independent techniques (*in situ* XRD synchrotron versus *ex situ* N₂ adsorption at 77 K, respectively), are very similar, providing a strong confirmation of the validity of the reported apparent activation energy of the surfactant-templating process. This apparent activation energy is in the order of that of the crystallization of zeolites,^[13] hence confirming that the mesostructuring of FAU zeolite is energetically feasible under the conditions of time and temperature used in the synthesis of zeolites, which opens new possibilities for the introduction of mesoporosity in zeolites using surfactants.

Experimental Section

Details on the experimental procedures, characterization and control experiments are given in the Supporting Information.

Acknowledgements

This work was supported by the Spanish MINECO (PCIN-2013-164) and the EC through the ERA-NET CAPITA (AEI/FEDER, project WAVES, EP7-NMP-266543) and the ALBA Synchrotron

(refs. 2016021622 and 2016021729). E.S. thanks the Spanish MINECO and AEI/FEDER, UE (CTQ2015-74494-JIN). E.S. and N.L. acknowledge the University of Alicante support (UATALENTO16-03 and UATALENTO17-05, respectively). The authors thank F. Fauth and C. Kamma-Lorger from the ALBA Synchrotron for helpful suggestions with the flow reactor design and assistance during the XRD and SAXS experiments, and J. Carpena and J.M. Martínez from the UA for assistance with the flow reactor design and construction.

Keywords: apparent activation energy; kinetics; mesoporous zeolites; surfactant-templating; synchrotron

- [1] C.T. Kresge, M.E. Leonowicz, W.J. Roth, J.C. Vartuli, J. S. Beck, *Nature* **1992**, 359, 710.
- [2] a) C. Perego, R. Millini, *Chem. Soc. Rev.* **2013**, 42, 3956. b) C. T. Kresge, W.J. Roth, *Chem. Soc. Rev.* **2013**, 42, 3663.
- [3] a) Y. Goto, Y. Fukushima, P. Ratu, Y. Imada, Y. Kubota, Y. Sugi, M. Ogura, M. Matsukata, *J. Porous Mater.* **2002**, 9, 43; b) I. I. Ivanova, E. E. Knyazeva, *Chem. Soc. Rev.* **2013**, 42, 3671; c) M. Choi, K. Na, J. Kim, Y. Sakamoto, O. Terasaki, R. Ryoo, *Nature* **2009**, 461, 246.
- [4] a) W. Park, D. Yu, K. Na, K.E. Jelfs, B. Slater, Y. Sakamoto, R. Ryoo, *Chem. Mater.* **2011**, 23, 5131; b) J. Kim, M. Choi, R. Ryoo, *J. Catal.* **2010**, 269, 219; c) M. Choi, H.S. Cho, R. Srivastava, C. Venkatesan, D.H. Choi, R. Ryoo, *Nat. Mater.* **2006**, 5, 718.
- [5] a) K. Li, M. Beaver, B. Speronello, J. Garcia-Martinez in *Mesoporous Zeolites* (Eds.: J.Garcia-Martinez, K. Li), Wiley-VCH, Weinheim, **2015**, pp. 321-348; b) A. Sachse, J. Garcia-Martinez, *Chem. Mater.* **2017**, 29, 3827.
- [6] a) J. García-Martínez, M. Johnson, J. Valla, K. Li, J. Ying, *Catal. Sci. Technol.* **2012**, 2, 987; b) J. García-Martínez, K. Li, G. Krishnaiah, *Chem. Commun.* **2012**, 48, 11841; c) J. García-Martínez, C. Xiao, K.A. Cychosz, K. Li, W. Wan, X. Zou, M. Thommes, *ChemCatChem* **2014**, 6, 3110; d) T. Prasomsri, W. Jiao, S.Z. Weng, J. García-Martínez, *Chem. Commun.* **2015**, 51, 8900.
- [7] N. Linares, A. Sachse, E. Serrano, A. Grau-Atienza, E. O. Jardim, J. Silvestre-Albero, M. A. Liuthevicene Cordeiro, F. Fauth, G. Beobide, O. Castillo, J. Garcia-Martínez, *Chem. Mater.* **2016**, 28, 8971.
- [8] K. Li, J. Valla, J. García-Martínez, *ChemCatChem* **2014**, 6, 46.
- [9] J.C. Groen, G.M. Hamminga, J.A. Moulijna, J. Pérez-Ramírez, *Phys. Chem. Chem. Phys.*, **2007**, 9, 4822.
- [10] A. Sachse, A. Grau-Atienza, E.O. Jardim, N. Linares, M. Thommes, J. García-Martínez, *Cryst. Growth Des.* **2017**, 17, 4289.
- [11] F. Kleitz, W. Schmidt, F. Schüth, *Micropor. Mesopor. Mater.* **2001**, 44-45, 95.
- [12] a) V.R. Choudhary, S.G. Pataskar, *Thermochimica Acta*, **1986**, 97 1; b) R.B. Borade, A. Clearfield, *Micropor. Mater.* **1996**, 5, 289.
- [13] S. P. Zhdanov, R. F. Gould, in: *Molecular Sieve Zeolites – I, Advances in Chemistry Series*, Vol. 101 (Eds.: S. P. Zhdanov, R. F. Gould), ACS, Washington, DC, **1971**, pp. 20–43; b) S. P. Zhdanov and N. N. Samulevich, in: *Proceedings of the Fifth International Conference on Zeolites* (Ed.: L. V. C. Rees), Naples, Heyden, London-Philadelphia-Rheine, **1980**, pp. 75–84; c) H. Kacirek, J.H. Lechert, *Phys. Chem.* **1976**, 80, 1291; d) B. J. Schoeman, J. Sterte, J.E. Otterstedt, *Zeolites* **1994**, 14, 568.
- [14] (a) A. Navrotsky, O. Trofymuk, A. A. Levchenko, *Chem. Rev.* **2009**, 109, 3885. (b) I. Petrovic, A. Navrotsky, M.E. Davis, S.I. Zones, *Chem. Mater.*, **1993**, 5, 1805.
- [15] I. I. Ivanova, E. E. Knyazeva, *Chem. Soc. Rev.* **2013**, 42, 3671.
- [16] J. D. Rimer, O. Trofymuk, A. Navrotsky, R. F. Lobo, D. G. Vlachos, *Chem. Mater.* **2007**, 19 (17), 4189.
- [17] D. Verboekend, G. Vilé, J. Pérez-Ramírez, *Cryst. Growth Des.* **2012**, 12, 3123.
- [18] O. Trofymuk, A. A. Levchenko, S. H. Tolbert, A. Navrotsky, *Chem. Mater.* **2005**, 17, 3772.

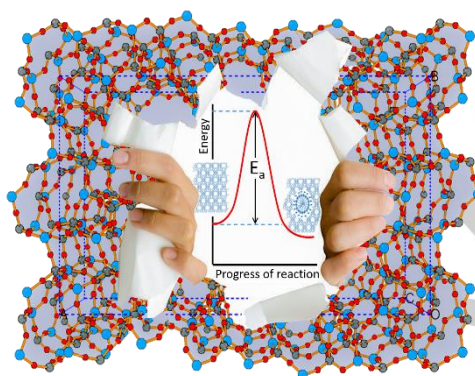
Entry for the Table of Contents (Please choose one layout)

Layout 1:

COMMUNICATION

Big pores, small energy:

Through the systematic study of the kinetics of the different processes involved in the mesopores formation in zeolites, we have confirmed that the mesostructuring of USY zeolite with surfactants can be realized under the conditions of time and temperature used in the synthesis of zeolites.



*N. Linares, E. O. Jardim, A. Sachse,
E. Serrano, J. García-Martínez**

Page No. – Page No.

**The energetics of mesopore
formation in zeolites with
surfactants**